Structure of SiO_2/4H-SiC interface probed by positron annihilation spectroscopy

M. Maekawa and A. Kawasuso
Advanced Science Research Center, Japan Atomic Energy Research Institute, Watanuki 1233, Takasaki, Gunma 370-1292, Japan

M. Yoshikawa and A. Miyashita
Takasaki Establishment, Japan Atomic Energy Research Institute, Watanuki 1233, Takasaki, Gunma 370-1292, Japan

R. Suzuki and T. Ohdaira
Photonics Research Institute, National Institute of Advanced Industrial Science and Technology, Tsukuba, Ibaraki 305-8568, Japan
(Received 13 June 2005; revised manuscript received 29 November 2005; published 23 January 2006)

The structure of the SiO_2/4H-SiC interface produced by dry oxidation has been studied using positron annihilation spectroscopy using energy-variable slow positron beams. Based on the Doppler broadening shape and wing parameter (*S*-*W*) correlation, the interface layer was clearly distinguished from the SiO_2 and SiC layers. A single positron lifetime of 451 ps, which is sufficiently longer than that in the SiC substrate ($\sim$140 ps) and close to the second lifetime in the SiO_2 layer, was obtained when the incident positron energy was adjusted at the interface layer. The electron-positron momentum distribution associated with the interface layer was well explained by a theoretical calculation that considered the annihilation of the positrons by the oxygen valence electrons in the SiO_2 layer. The annealing process after the oxidation resulted in the modification of the electron-positron momentum distribution in a manner similar to that of the interface traps, thereby suggesting that the interface traps correlate with the positron annihilation site.

DOI: 10.1103/PhysRevB.73.014111 PACS number(s): 68.35.Ct, 78.70.Bj, 68.03.Hj, 71.15.Dx

I. INTRODUCTION

Silicon carbide (SiC) is a promising material for high-power electronic devices. The oxide layer can be grown using conventional oxidation methods; therefore, SiC is suitable for fabricating high-power metal-oxide-semiconductor (MOS) devices.[1] However, the channel mobility of the electrons between the source and drain of the MOS devices is still lower than that expected from the ideal SiC electron mobility.[2–4] Capacitance-voltage (*C*-*V*) measurements indicate that the interface states that are located in the range of 0.1–0.2 eV below the conduction band edge (E_c) result in the low mobility.[5–7] The interface trap density can be reduced by postoxidation annealing (POA).[8–11] In order to reveal the origin of the interface traps, many extensive studies have been performed, such as electron spin resonance (ESR),[12] spectroscopic ellipsometry (SE),[13,14] x-ray photoelectron spectroscopy (XPS),[15–17] photoemission spectroscopy (PS),[18,19] and infrared absorption (IR).[20] The results of these studies suggest the existence of a SiO_2/4H-SiC interface layer that contains irregularities such as suboxides, silicon and carbon dangling bonds, carbonclusters, and so on. The correlation between the above-mentioned irregularities and interface traps has not been fully elucidated.

Positron annihilation spectroscopy (PAS) enables the study of vacancy defects in materials,[21,22] and it can be used for the detection of vacancy defects in the subsurface.[23] The defects and microvoids at the SiO_2/Si interface was detected by PAS.[24–29] Positronium (Ps) formation occurs when positrons are trapped at the microvoids, and it is suppressed when positrons preferentially annihilate at competitive centers such as dangling bonds. It is also reported that a crystalline SiO_2 layer could exist at the SiO_2/Si interface. However, in the case of the SiO_2/SiC interface, no evidence of the formation of crystalline SiO_2 has been obtained. Recently, PAS was also applied to study the SiO_2/4H-SiC interface.[30–32] The motion of positrons under an electric field was examined by using MOS structures.[30,31] It was confirmed that positrons respond to the band bending generated due to the internal field effects. The effect of POA was also systematically studied using the Doppler broadening technique.[32] The annihilation characteristics of the positron traps in the SiO_2/4H-SiC interface layer are observed to be similar to those of the SiO_2/Si interface. However, the detailedchemical environment of the positron annihilation site and the Ps formation process have not been clarified. Therefore, coincidence Doppler broadening (CDB) and positron lifetime measurements are required to investigate these aspects.

In this study, we focused on the structure of the interface layer of the SiO_2/4H-SiC produced by conventional dry oxidation. A detailed study of the structure and chemical environment of positron annihilation sites in the interface layer was carried out using Doppler broadening, positron lifetime, and first-principles calculations. The correlation between interface traps detected by *C*-*V* measurement and positron annihilation centers through POA were also examined.

II. EXPERIMENT

The samples used in this study were cut from an *n*-type chemical-vapor-deposition (CVD)-grown 4H-SiC epilayer with a thickness of 5 μm on an 8°-off oriented 4H-SiC(0001) substrate purchased from CREE Research Inc. The epitaxial layer was doped with nitrogen and the net donor concentration was approximately 5×10^{15} cm^{-3}. These

samples were oxidized in dry oxygen ambient at 1200 °C for 3 h. The oxide thickness was approximately 40 nm.[33] Postoxidation (isochronal) annealing was conducted in argon ambient from 400 to 1100 °C for 3 h.

The Doppler broadening of annihilation radiation (511 keV) was measured as a function of the incident positron energy (E) from 0.2 to 20 keV at room temperature. The obtained Doppler spectra were characterized by S and W parameters, which are defined as the peak and tail intensities, respectively, of the Doppler spectrum. The windows for S and W parameters were 510.2 to 511.8 keV and 513.6 to 514.5 keV, respectively. All the S and W parameters were normalized to those in the SiC epilayer. In order to ascertain the chemical environment at the positron annihilation site in detail, the CDB measurement, which enables the enhancement of the peak-to-background ratio,[34,35] was also carried out. In each CDB spectrum, 2×10^7 counts were accumulated. In addition, positron lifetime measurement was performed at room temperature using a pulsed positron beam with energies of 0.8, 3.7, and 15 keV.[36] The time resolution was 260 ps in full width at half maximum (FWHM). In each positron lifetime spectrum, 5×10^6 counts were accumulated. The obtained positron lifetime spectra were analyzed using the PATFIT-88 program.[37]

III. THEORETICAL CALCULATION

In order to interpret the obtained positron annihilation characteristics, the Doppler broadening of annihilation radiation and positron lifetimes were calculated within the local density approximation.[22] The valence electron-positron momentum distribution was computed using the conventional scheme

$$\rho_v(\mathbf{p}) = \pi r_e c^2 \sum_n \left| \int e^{-i\mathbf{pr}} \Psi_+(\mathbf{r}) \Psi_n(\mathbf{r}) \sqrt{\gamma(\mathbf{r})}\, d\mathbf{r} \right|^2, \quad (1)$$

where r_e is the classical electron radius; c, the velocity of light; $\Psi_+(\mathbf{r})$, the positron wave function; $\Psi_n(\mathbf{r})$, the valence electron wave function of the nth band; and $\gamma(\mathbf{r})$, the enhancement factor. The summation goes over all the occupied bands. For core electrons, Alatalo's manner was employed[38]

$$\rho_c(\mathbf{p}) = \pi r_e c^2 \sum_{i,nlm} \left| \int e^{-i\mathbf{pr}} \Psi_+(\mathbf{r}) \Psi_{i,nlm}(\mathbf{r}-\mathbf{R}_i) \sqrt{\gamma(\mathbf{r})}\, d\mathbf{r} \right|^2, \quad (2)$$

where $\Psi_{i,nlm}(\mathbf{r}-\mathbf{R}_i)$ represents the core electron wave function specified by the principal, azimuthal, and magnetic quantum numbers (nlm) of the ith atom and $\mathbf{R}_i$ denotes the position vector. Clementi and Roetti femtosecond (fs) analytical form for core electron wave functions was used.[39] The total momentum distribution is given by $\rho(\mathbf{p})=\rho_v(\mathbf{p})+\rho_c(\mathbf{p})$. The one-dimensional angular correlation of positron annihilation radiation (1D-ACAR) spectra was subsequently obtained by integrating $\rho(\mathbf{p})$ in two (p_y,p_z) momentum axes. The Doppler broadening spectra were obtained by convoluting the 1D-ACAR spectra with the Gaussian resolution function of the measurement system. The FWHM of the Gaussian function was assumed to be 4 mrad. The positron lifetime (inverse of the annihilation rate) was obtained by integrating the momentum density in the entire momentum space

$$\tau^{-1} = \int \rho(\mathbf{p})\, d\mathbf{p}. \quad (3)$$

For the calculation of the 4H-SiC crystal, a supercell containing 48 Si and 48 C atoms was constructed. The structure of an amorphous SiO_2 bulk was obtained by applying the simulated annealing method in the first-principles molecular dynamics approach as follows. A periodic cell of β-quartz containing 24 Si and 48 O atoms was used as the base structure. After adjusting the cell size to $10.48\times9.08\times11.44$ Å which corresponded to the density of an amorphous SiO_2 (2.2 g/cm^3), the temperature of the system was maintained at 4000 K for 3 ps and subsequently quenched to 300 K at the rate of 1000 K/ps. This amorphous SiO_2 structure was calculated using the Vienna *ab initio* simulation package (VASP) code.[40] The generalized gradient approximation (GGA) was used as the exchange-correlation functional. The time step was 1 fs. The average bond lengths of Si-O, Si-Si,and O-O were 1.62, 3.17, and 2.62 Å, respectively. These values are in good agreement with the experimental and other theoretical calculations.[41] Both the Boroński–Nieminen (BN) formula and the insulator model by Puska were tested at $\gamma(\mathbf{r})$.[42,43] The valence electron wave function was computed using the free-distributed ABINIT 4.1.4 code based on the norm-conserving pseudopotential method.[44] By considering the correlation interaction between a positron and electrons and the Coulomb interaction from ion cores, a self-consistent positron wave function was calculated based on the two component density functional theory in order to minimize the energy functional.[42] For the amorphous SiO_2 bulk and the 4H-SiC crystal, the cutoff energies of the plane wave basis set were 60 and 90 Ry, respectively.

IV. RESULTS AND DISCUSSION

A. As-oxidized state

Figure 1(a) shows the S-E plot obtained after oxidation. With increasing E, the S parameter first increases at $E=1$ keV and decreases to a constant value at $E>15$ keV. The S parameter at $E=1$ keV corresponds to the annihilation of positrons in the SiO_2 layer and the constant S parameter at $E>15$ keV reflects the positron annihilation in the SiC layer. At $E=3-10$ keV, the S parameter does not steeply decrease to its value in the SiC layer and shows a rather long tail. As seen in Fig. 1(b), the W parameter is fairly pronounced at around $E=3$ keV, and it gradually approaches its value in the SiC layer with increasing E in a manner similar to the S parameter. The inset in Fig. 1 shows the corresponding S-W plot. Apart from $(S,W)=(1.00,1.00)$ for the SiC layer and $(S,W)=(1.11,1.03)$ for the SiO_2 layer, there exists another distinguishable region at around $(S,W)=(1.03,1.18)$. This region is attributed to the SiO_2/4H-SiC interface layer.[32] Both S and W parameters gradually decrease to the bulk values at $E>3$ keV. It is physically difficult to assume that the interface layer spreads itself into such a deep region

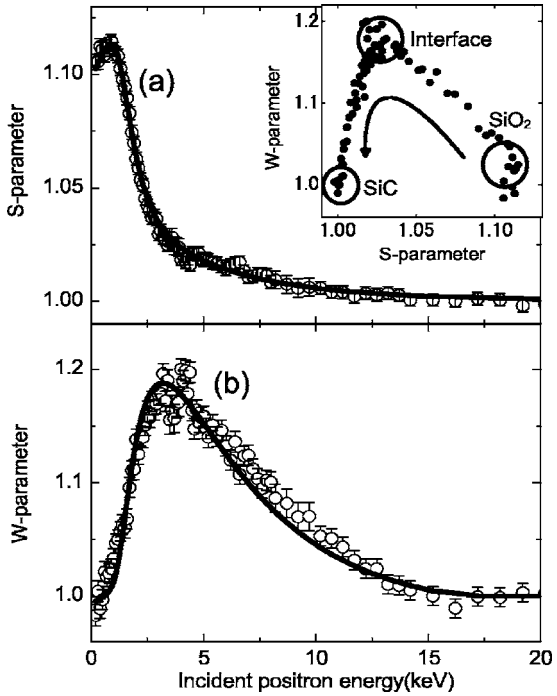

FIG. 1. Open circles are Doppler broadening (a) S parameter and (b) W parameter for the as-prepared SiO_2/4H-SiC sample as a function of incident positron energy. The inset shows the corresponding S-W plot. Both S and W parameters are normalized to their average values obtained at high energy regions ($E>16$ keV). Solid lines are the best fittings by the VEPFIT code.

(~500 nm). The band bending causes a part of the positrons implanted in the relatively deep region to drift back to the interface. In reality, the C-V measurements showed the formation of an electron depletin region at the interface between SiO_2 and n-type 4H-SiC. Therefore, for the positive particles, a drift field from the SiC layer to the interface layer is generated.[30]

The above-mentioned S-E and W-E plots were analyzed considering one-dimensional positron diffusion. The probability of the presence of positrons at the depth z $[n(z)]$ is given by

$$\frac{d^2n(z)}{dz^2} - \frac{e}{kT}\frac{dn(z)\mathcal{E}(z)}{dz} - \frac{n(z)}{L(z)^2} + \frac{P(z,E)}{D} = 0, \qquad (4)$$

where k is the Boltzmann constant; T, the temperature; e, the elementary electric charge; and $\mathcal{E}(z)$, the electric field. In addition, $L(z)$, $P(z,E)$, and D are the diffusion length, implantation profile, and diffusion constant of positrons, respectively.[45] $L(z)$ is further given by $L(z)=(D\tau_{\mathrm{eff}})^{1/2}$, where τ_{eff} is the effective positron lifetime $\{=1/[1/\tau_b(z)+\kappa(z)]$, where $\tau_b(z)$ is the bulk positron lifetime and $\kappa(z)$ is the positron trapping rate by the defects$\}$. $P(z,E)$ is given by

$$P(z,E) = \exp\left[-\left(\frac{z}{z_0}\right)^m\right], \qquad (5)$$

where z_0 is given by

$$z_0 = \frac{\langle z\rangle}{\Gamma\left(\frac{1}{m}+1\right)}. \qquad (6)$$

In this study, the value of m was fixed at 2.[46] Assuming that the system is described as the thin layers where individual layers have their own $S(W)$ parameters, the obtained $S(W)$ parameter is given by

$$S(E) = \sum_j F_j(E)S_j, \quad W(E) = \sum_j F_j(E)W_j \qquad (7)$$

where S_j and W_j are the S and W parameters of jth layer, respectively, $F_j(E)$ is the fraction of positrons that annihilate in the jth layer $[\Sigma_j F_j(E)=1]$. In the present case, the structure of this SiO_2/4H-SiC sample may be modeled as the combination of four layers, SiO_2 surface, SiO_2 layer, SiO_2/4H-SiC interface layer, and SiC layer. Furthermore, the SiC layer is divided into a depletion region, in which an electric field exists, and a field-free bulk region. Therefore, the value of j is 5. The S-E and W-E relationships are obtained by solving the above-mentioned diffusion equation. Optimum S-E and W-E relationships can be obtained with least square fitting using the variable fitting parameters S_j, W_j, $L(z)$, $\mathcal{E}(z)$, and layer thickness Δ_t. The analysis was carried out using the VEPFIT code.[45] First, the fitting of the S-E plot was carried out by fixing $L(z)$, $\mathcal{E}(z)$, and Δ_t to predicted values, and the S parameters were obtained. Next, these S parameters were used in the fitting $L(z)$, $\mathcal{E}(z)$, and Δ_t. This procedure was repeated until optimal parameters were determined within physically permitted ranges. Using these values, the fitting of the W-E plot was carried out by selecting only W as the fitting parameter. The solid lines in Fig. 1 are the obtained best fittings. Table I summarizes the parameters obtained in the fitting procedure. The S and W parameters in the interface layer are obtained as 1.02 and 1.16, which correspond to the interface layer of the S-W plot in Fig. 1. The layer thickness of SiO_2 (45 nm) is in reasonable agreement with that expected based on the oxidation rate. The width of the interface layer obtained as 3.9 nm is in agreement with that reported using other techniques.[20] The width of the depletion layer was in good agreement with that obtained from the C-V measurements (~120 nm). The electric field was stronger than that of the SiO_2/Si interface (2–3 keV/cm).[46] This may reflect the fact that more defects exist in the SiO_2/4H-SiC interface layer compared to those in the SiO_2/Si interface. Even if an electric field did exist in the interface layer, it barely contributed to the fitting results due to its thickness. The obtained diffusion length of the SiC layer (221 nm) is comparable to the typical values obtained in defect-free crystals. The short diffusion length in the SiO_2 layer may be caused by the preferential Ps formation at the microvoids.[47] The diffusion length in the interface layer is also negligibly short compared to that in the other layer. This indicates that the interface layer can be treated as a perfect absorber for positrons, i.e., there are many defects at the SiO_2/4H-SiC interface layer that prevent positron transmission to the SiO_2 layer.

TABLE I. S and W parameters, layer thicknesses (Δ_t), diffusion lengths (L) and electric fields ($\mathcal{E}$) obtained from the analyses of SiO_2/4H-SiC samples before and after the postoxidation annealing. SiO_2 surface has no finite width. SiC layer has a semi-infinite depth.

Region	S	W	Δ_t(nm)	L(nm)	$\mathcal{E}$(kV/cm)
		As-oxidized			
SiO_2 surface	1.10±0.005	0.99±0.004			
SiO_2	1.13±0.008	1.00±0.009	45±5	10.6±1.0	
SiO_2-SiC interface	1.02±0.005	1.25±0.01	3.9±3	1.8±0.2	
SiC(depletion)	1.00(fixed)	1.00(fixed)	95±3	221±20	5.4±0.1
SiC(bulk)	1.00(fixed)	1.00(fixed)	Semi-infinite	221±15	
		Postoxidation annealing			
SiO_2 surface	1.10±0.005	0.99±0.004			
SiO_2	1.16±0.011	0.93±0.004	46.8±5	9.6±1.2	
SiO_2-SiC interface	1.02±0.002	1.17±0.008	2.1±2	1.8±0.1	
SiC(depletion)	1.00(fixed)	1.00(fixed)	95±4	221(fixed)	2.73±0.05
SiC(bulk)	1.00(fixed)	1.00(fixed)	Semi-infinite	221(fixed)	

Figure 2 shows the CDB spectra for the SiO_2/4H-SiC interface layer and the SiC layer. The theoretical CDB spectrum and the contribution of individual core electrons to SiC are also depicted. The experimental result is in good agreement with that obtained theoretically. It was also confirmed that the calculated positron lifetime is 139 ps, which is also comparable to the value of the lifetime obtained experimentally.[21] In order to observe the fine structures in the CDB spectrum of the interface, it was divided by the spectrum of the SiC layer. This resulted in a ratio spectrum such as that shown in Fig. 3.The intensity at $p=10-15$ mrad is greater than unity and it causes the high W parameter in the interface layer in Fig. 1(b). The enhancement of the CDB intensity in this region is probably caused by the smearing of the momentum distribution because of the lack of translational symmetry and/or the influence of particular electron momenta. These two possibilities will be discussed later in further detail along with the theoretical calculations.

Figure 4 shows the positron lifetimes and intensities in the SiO_2 layer ($E=0.8$ keV), SiO_2/4H-SiC interface layer ($E=3.7$ keV), and SiC layer ($E=15$ keV). In order to evaluate

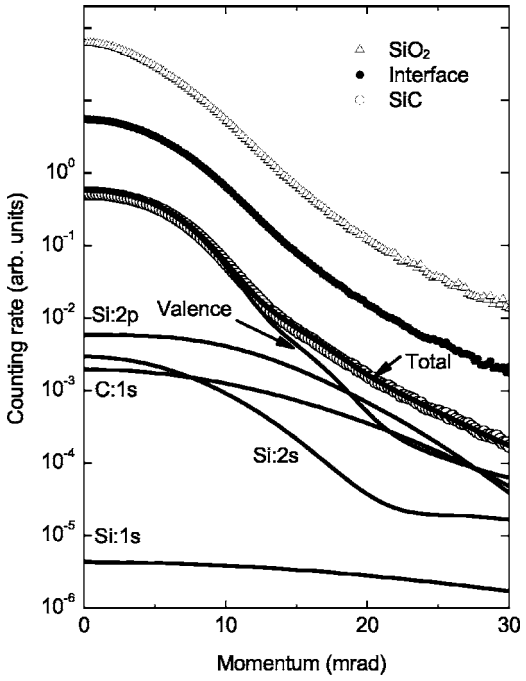

FIG. 2. Coincidence Doppler broadening spectra obtained for the interface ($E=3.7$ keV) and SiC ($E=15$ keV) layers of the as-prepared SiO_2/4H-SiC sample. Note that 1 keV Doppler shift corresponds to 3.92 mrad and 0.154 a.u. Theoretical CDB spectrum and contribution of individual shells for 4H-SiC are also demonstrated as solid lines.

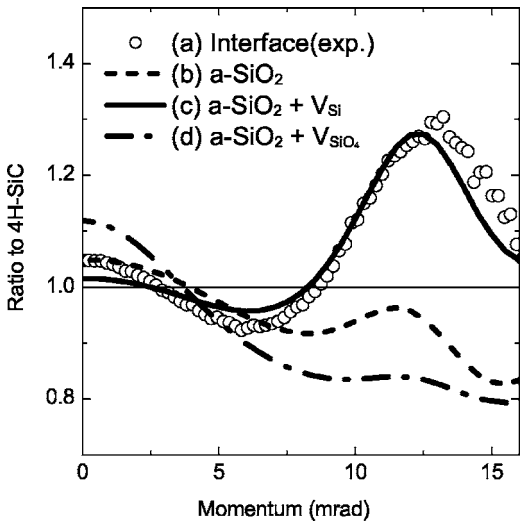

FIG. 3. Differential CDB spectra for the interface layer of the as-prepared SiO_2/4H-SiC sample shown in Fig. 2 [$N(p)/N_{SiC}(p)$, where $N_{SiC}(p)$ denotes the CDB spectrum for the SiC layer shown in Fig. 2]. Broken, solid, and chained lines represent the calculated ratio curves for the amorphous SiO_2 (a-SiO_2), silicon vacancy and SiO_4 vacancy in (a-SiO_2), respectively.

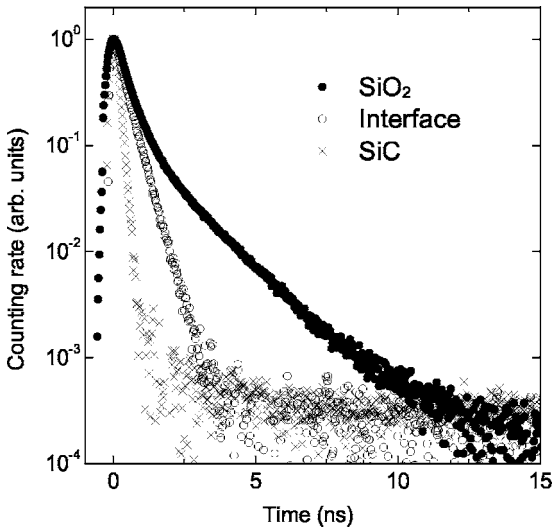

FIG. 4. Positron lifetime spectra obtained for the SiO_2 (E =0.8 keV), interface (E=3.7 keV) and SiC (E=15 keV) layers of the as-prepared SiO_2/4H-SiC sample.

only the SiO_2 layer, positron implantation energy was set to E=0.8 keV to completely stop all the positrons in SiO_2 layer. The positron lifetime spectra obtained from individual layers were rather different, thereby suggesting different open volumes. These lifetime spectra were analyzed using a multiexponential function: $L(t)=\Sigma I_i \exp(-t/\tau_i)/\tau_i$, where τ_i and I_i are the lifetimes and intensities ($\Sigma I_i=100\%$), respectively. Table II shows the results of above-mentioned analyses.

In porous materials such as SiO_2, characteristic Ps lifetimes are observed.[48] Since Ps represents the bound state of a positron and a electron, it exists in the spin parallel "ortho" state as well as the spin antiparallel "para" state whose intrinsic lifetimes are 142 ns and 125 ps, respectively. The lifetime of the ortho-Ps is shortened to several nanoseconds depending on the size of the microvoids.[49] In the SiO_2 layer, when τ_1 is fixed to the lifetime of para-Ps (τ_1=125 ps), two more lifetime components, i.e., τ_2=472 ps and τ_3=1610 ps, are resolved. In the SiC layer, only one lifetime component τ_1=139 ps appears. This lifetime is in good agreement with that for the bulk SiC reported previously.[21] In the interface layer, only one lifetime component, τ=451 ps, is obtained. Neither the short lifetime observed in the SiC and SiO_2 layers nor the long lifetime (τ_3) in the SiO_2 layer appears to suggest that the interface layer is not a simple admixture between SiO_2 and SiC. The interface structure is expected to be analogous with the open-volume structure of the SiO_2 layer because a lifetime of 451 ps is similar to the second lifetime in the SiO_2 layer. According to the Makhovian implantation profile of positrons with an energy E=3.7 keV, 23% of the positrons are implanted into the SiC(bulk) layer, 6% annihilate in the SiO_2 layer, and the rest are implanted into the interface layer or the depletion layer.[50] Half of the positrons implanted into the SiC (bulk) diffuse into the depletion layer. Most positrons in the depletion layer are driven toward the SiO_2/SiC interface layer by the electric field because a positron can easily migrate under the influence of an electric field. The drift distance of the positrons in the depletion layer within their lifetime in SiC ($\sim$140 ps) is estimated to be several microns; this implies that these positrons reach the SiO_2/SiC interface layer. Although the remaining positrons annihilate in the SiC (bulk) layer, this positron lifetime component was not entirely separated due to the low intensity and short lifetime. Therefore, the lifetime in the SiC is hardly observable. Based on the results of the lifetime measurement of the SiO_2 layer, approximately 20% intensity was considered to be due to an amorphous network and 60% intensity was due to ortho-Ps. Hence, the total intensity of 1.2% is due to the amorphous network. This lifetime is not separated because it is close to the lifetime in an interface. Although the intensity of ortho-Ps is estimated to be 3.6%, even this component is scarcely separated because of the poor signal-to-noise ratio. Thus, the observed single lifetime is intrinsic to the interface.

For the SiO_2 layer, the high S parameter, low W parameter, and long positron lifetime are simply explained by considering the Ps formation. Due to para-Ps self-annihilation, the Doppler broadening spectra becomes narrow and results in a high S parameter.[51] The third lifetime component (τ_3 =1610 ps) arises from the pick-off annihilation of ortho-Ps, and the second lifetime component (τ_2=472 ps) may arise from the annihilation of positrons in the open-volume structure of the SiO_2 amorphous network of the SiO_2 layer.[52–54]

For the SiO_2/4H-SiC interface layer, only a single long lifetime, which is close to the second lifetime in SiO_2, appears. This result shows that the interface layer also has an open-volume structure similar to the SiO_2 layer. However,

TABLE II. Positron lifetimes and their intensities obtained for SiO_2/4H-SiC samples in the as-prepared state and after POA with various incident positron energies.

E(keV)	Region	τ_1(ps)	τ_2(ps)	τ_3(ps)	I_1(%)	I_2(%)	I_3(%)
			As-oxidized				
0.8	SiO_2	125(fixed)	472±2	1610±5	20.0±0.2	20.5±0.2	59.5±0.2
3.7	SiO_2-SiC interface		451±1			100	
15	SiC	139±1			100		
			Post-oxidation annealing				
0.8	SiO_2	125(fixed)	486±3	1477±3	19.1±0.2	12.0±0.3	68.9±0.2
3.7	SiO_2 SiC interface		462±1			100	
15	SiC	139±1			100		

the *S* parameter is even less than that of the Si monovacancy in SiC.[21] Moreover, the *W* parameter is too large to attribute it to simple vacancy defects. This contradiction may have two explanations. One is that the chemical environments of the positron annihilation sites are different for the Si and C atoms. Oxygen valence electrons possess higher momenta because of their compact wave function.[55–60] If positrons preferentially annihilate with oxygen valence electrons, the low *S* and high *W* parameters can be explained. The other is the effect of the second Brillouin (Jones) zone. In tetrahedral semiconductors, eight valence electrons completely occupy the second Brillouin zone and free positrons exist in a Bloch state. Therefore, in the Doppler spectrum, a discontinuous distribution appears at this boundary, as seen in the CDB spectrum of the 4H-SiC layer in Fig. 2.[60–62] When positrons are localized at vacancy defects, the effect of the second Brillouin zone tends to vanish due to the lack of translational symmetry. Consequently, in the ratio spectrum, a bump may appear at the second Brillouin zone boundary and the *W* parameter will increase if the window is set around it. These possibilities are examined by comparing the theoretical calculation with appropriate models as follows.

Since the lifetime in the interface layer resembles τ_2 of the SiO_2 layer, the positron annihilation characteristics in an amorphous SiO_2 layer were initially simulated. The calculated positron lifetime in the amorphous SiO_2 bulk is 581 ps based on the insulator model.[43] This lifetime is longer than the observed lifetime (472 ps). However, it is rather problematic to compare these theatrical and experimental lifetimes, since in the amorphous SiO_2 not only free positron annihilation but also Ps annihilation may contribute to the second component.[28,63] The calculated CDB ratio curve for the amorphous SiO_2 bulk is shown in Fig. 3(b). However at $p=10-15$ mrad, the intensity is rather weak compared to that observed in the experiment. Therefore, the experimental CDB ratio curve can hardly be explained by only considering a simple amorphous SiO_2 bulk. In order to reproduce the observation, it may be required to consider a strong interaction between positrons and oxygen valence electrons.

Although the effect of Ps formation should be considered in the SiO_2 layer, when the positrons localize to the defects, comparatively exact lifetime calculations is possible due to no Ps formation. Since there is no Ps formation in the interface layer, comparison of an experiment value and a calculation value is effective. To enhance the annihilation probability with oxygen valence electrons in the amorphous SiO_2 bulk, the calculation for a silicon vacancy (V_{Si}) was performed. For comparison, a SiO_4 vacancy (V_{SiO_4}) at which positrons mainly annihilate with silicon valence electrons, was also examined. A schematic drawing of these defects is shown in Fig. 5. The reason due to which V_{SiO_4} is considered instead of oxygen vacancy (V_O), is the weak localization of the positron wavefunction at V_O. During preliminary calculations, the remarkable differences in the momentum distributions and lifetimes were not observed by the artificial relaxation. Hence, all the calculations were performed with an ideal geometry. Only the neutral charge state was considered. In Figs. 3(c) and 3(d), the theoretical ratio spectra for V_{Si} and V_{SiO_4} are shown. In the case of V_{SiO_4}, the ratio curve is not compatible with the experiment. The intensity at $p=10-15$ mrad is particularly weak, whereas in the case of V_{Si}, the intensity at $p=10-15$ mrad increased sufficiently and the curve shape was rather similar to the experimental curve. It is also observed that the intensity around $p=0$ mrad is significantly suppressed. This is also consistent with the observed low *S* parameter. For the further systematic examination of the effect of the oxygen dangling bonds, $V_{SiO_x}(x=1-3)$ where the number of oxygen dangling bonds decreases with *x*, was simulated. It was observed that the intensity at $p=10-15$ mrad increased with the increasing number of oxygen dangling bonds. In addition, the calculated lifetimes of positrons trapped at V_{Si}, V_{SiO}, V_{SiO_2}, V_{SiO_3}, and V_{SiO_4} are 469, 484, 486, 740, and 948 ps, respectively; the values were obtained based on the insulator model. The lifetime of V_{Si} is in reasonable agreement with the observed lifetime of 451 ps. It is probable that the positrons preferentially annihilate at the voids that contain the oxygen dangling bonds in the SiO_2 amorphous network. Positron lifetimes of V_{Si}, V_{SiO}, V_{SiO_2} are shorter than that of bulk value. This phenomena is due to the fact that the annihilation of positrons with oxygen valence electrons occurs preferentially at V_{Si}. The local valence electron density at the vacancy where the positron wavefunction is localized becomes higher than that of the bulk. A similar tendency is also observed in the calculation using the atomic superposition method.[64]

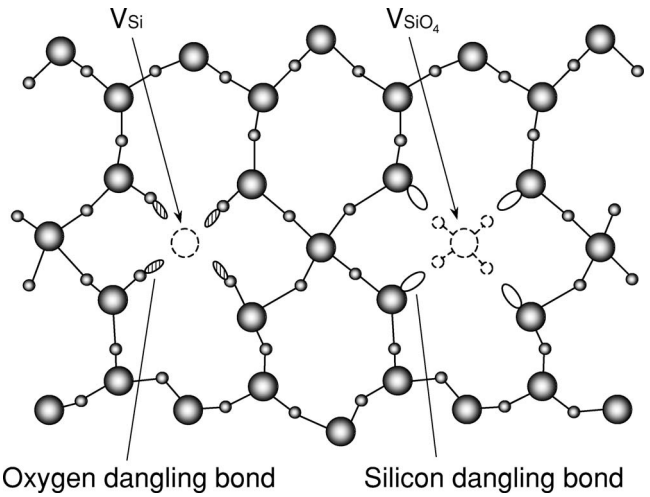

FIG. 5. The schematic drawing of the atomic structure of V_{Si} and V_{SiO_4}.

B. Effect of postoxidation annealing

Figure 6 shows the *S*-*E* and *W*-*E* curves for the SiO_2/4H-SiC samples annealed at 950 °C for 3 h. The *S* and *W* parameters in each layer, the layer thickness, and the diffusion length obtained from the VEPFIT analyses along with the lifetimes and their intensities are summarized in Tables I and II.

The *S* (*W*) parameters in the SiO_2 layer increase (decrease) by POA. The individual lifetimes in the SiO_2 layer do not change significantly by POA. However, the Ps fraction (I_1+I_3) increases; hence, the second intensity (I_2) relatively

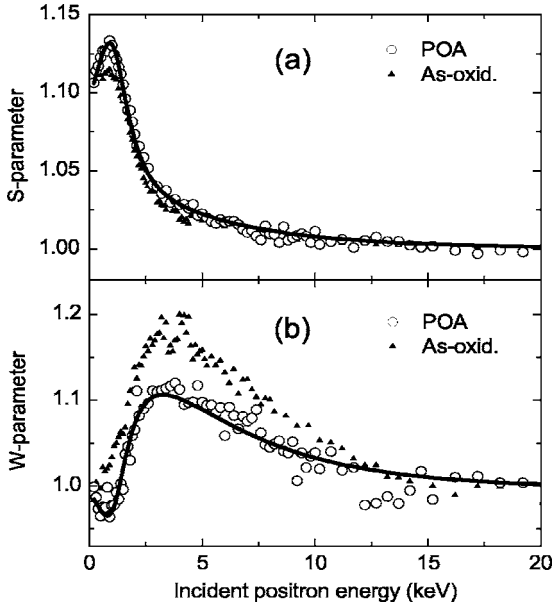

FIG. 6. Open circles are Doppler broadening (a) S parameter and (b) W parameter for the SiO_2/4H-SiC sample after POA treatment as a function of incident positron energy. Both S and W parameters are normalized to their average values obtained at high energy regions ($E > 16$ keV). For references, S and W parameters obtained for the as-prepared states are also shown. Solid lines are the best fittings by the VEPFIT code.

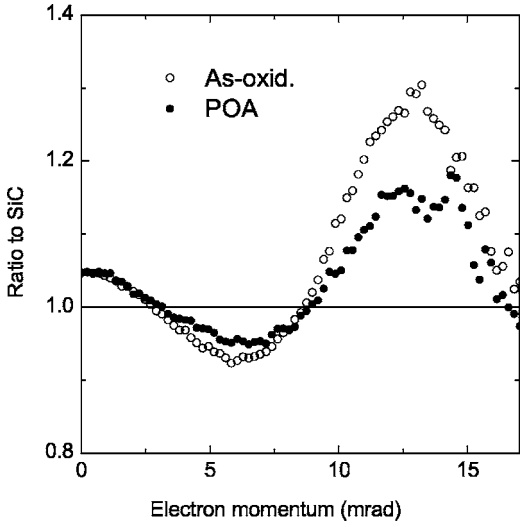

FIG. 7. Differential CDB spectra $[N(p)/N_{SiC}(p)]$ for the SiO_2/4H-SiC interface before and after POA treatment. $N_{SiC}(p)$ denotes the CDB spectrum for SiC layer shown in Fig. 2.

decreases. These observations indicate that the Ps formation in the SiO_2 layer is enhanced after POA. It is possible that in the as-prepared state, certain competitive positron trapping centers for Ps formation exist and these are recovered by POA.

At the interface, both the S parameter and lifetime remain unchanged, while the W parameter significantly decreases by POA. This situation is also observed in the CDB ratio spectrum, as shown in Fig. 7, where the bump at $p = 10-15$ mrad decreases by POA. These results suggest that porous structures of the interface layer are scarcely affected by POA but the number of oxygen dangling bonds at the positron annihilation site decreases. This is purely a thermal effect since the POA was conducted in dry argon ambient.

Isochronal annealing was carried out to investigate whether the change of W parameter related to the oxygen dangling bonds has a correlation with the interfacial defects that give rise to the interface traps. The number of interface traps per unit area is determined by the C-V measurements after forming the gate and Ohmic electronode for the MOS structures. Figure 8 shows the comparison of the annealing behavior of the W parameter with the integrated interface trap density in the band gap obtained from the C-V measurements. The interface traps begin to decrease dramatically at approximately 600 °C. It is observed that the W parameter also decreases in the same temperature range. It is inferred that the recovery of interfacial defects is accompanied with the rearrangement of the oxygen dangling bonds where positrons annihilate. In the other types of measurements, such as, Fourier-transform infrared (FTIR), ellipsometry, and XPS, it is observed that the reductions in suboxides and/or Si dangling bonds, which remain at the SiO_2/4H-SiC interface layer, occur during the POA process.[8,65–67] On abruptly halting the oxidation, the suboxides formed in the interface layer[19,68] and the unreacted oxygen atoms were frozen. Such oxygen atoms migrate to the interface on additional heating[69] and the suboxides may be reoxidized. Thus, the reduction of the positron annihilation probability of oxygen valence electrons by POA is explained well by the re-oxidation process that occurs at the interface.

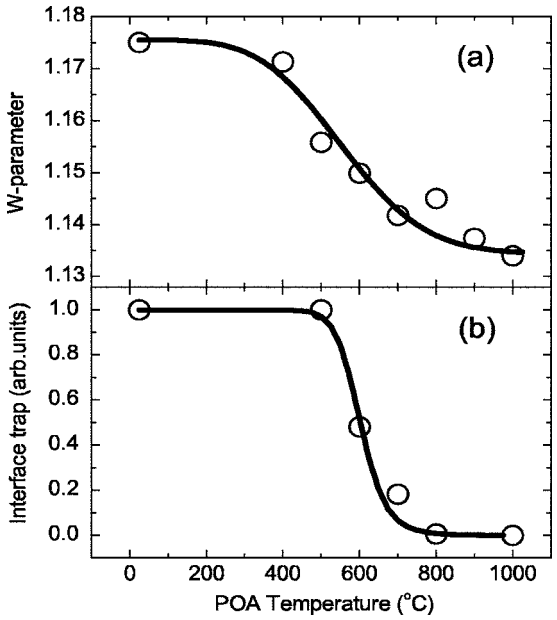

FIG. 8. Interface trap density obtained from the capacitance-voltage measurements and Doppler broadening W parameter as a function of annealing temperature. Annealing duration at each temperature is 3 h.

V. SUMMARY

The structure at the SiO_2/4H-SiC interface prepared by the dry oxidation method has been studied using positron annihilation measurements. It was found that an interface layer with a thickness of a few nanometers exists between the SiO_2 and SiC layers. The positrons implanted in the SiC layer drift toward the interface layer due to the internal electric field. The measurement of the positron lifetime indicates that the interface layer is rather porous. It was observed that positrons preferentially annihilate with the oxygen valence electrons. The annihilation fraction with the oxygen valence electrons decreased due to POA at approximately 600 °C. The interface trap density detected by the *C-V* measurement decreased in the same temperature range. These phenomena occur simultaneously with the reoxidation of the suboxide layer because of the migrating atoms during the POA process.

ACKNOWLEDGMENT

We thank Dr. Ohnuma of Central Research Institute of Electric Power Industry for calculating the atomic structure of amorphous SiO_2.

*Electronic address: maekawa@taka.jaeri.go.jp

[1] G. Pensl and W. Choyke, Physica B **185**, 264 (1993).
[2] V. V. Afanas'ev, M. Bassler, G. Pensl, and A. Stesmans, Mater. Sci. Forum **389-393**, 961 (2002).
[3] K. Fukuda, J. Senzaki, M. Kushibe, K. Kojima, R. Kosugi, S. Suzuki, S. Harada, T. Uzuki, T. Tanaka, and K. Arai, Mater. Sci. Forum **389-393**, 1057 (2002).
[4] T. Iida, Y. Tomioka, H. Yaguchi, M. Yoshikawa, Y. Ishida, H. Okumura, and S. Yoshida, Jpn. J. Appl. Phys., Part 2 **39**, L1054 (2000).
[5] S. Suzuki, S. Harada, R. Kosugi, J. Senzaki, W. J. Cho, and K. Fukuda, J. Appl. Phys. **92**, 6230 (2002).
[6] S. Harada, R. Kosugi, J. Senzaki, W. J. Cho, K. Fukuda, K. Arai, and S. Suzuki, J. Appl. Phys. **91**, 1568 (2002).
[7] M. K. Das, B. S. Um, and J. A. C. Jr, Mater. Sci. Forum **338-342**, 1069 (2000).
[8] M. Yoshikawa, M. Satoh, T. Ohshima, and H. Itoh, Mater. Sci. Forum **389-393**, 1009 (2002).
[9] J. Senzaki, K. Kojima, S. Harada, R. Kosugi, S. Suzuki, T. Suzuki, and K. Fukuda, Jpn. J. Appl. Phys., Part 2 **40**, L1201 (2001).
[10] K. Fukuda, W. J. Cho, K. Arai, S. Suzuki, J. Senzaki, and T. Tanaka, Appl. Phys. Lett. **77**, 866 (2000).
[11] G. Y. Chung, C. C. Tin, J. R. Williams, K. McDonald, M. D. Ventra, S. T. Pantelides, L. C. Feldman, and R. A. Weller, Appl. Phys. Lett. **76**, 1713 (2000).
[12] J. Isoya, R. Kosugi, K. Fukuda, and S. Yamasaki, Mater. Sci. Forum **389-393**, 1025 (2002).
[13] Y. Tomioka, T. Iida, M. Midorikawa, H. Tukada, K. Yoshimoto, Y. Hijikata, H. Yaguchi, M. Yoshikawa, Y. Ishida, R. Kosugi, and S. Yoshida, Mater. Sci. Forum **389-393**, 1029 (2002).
[14] L. Chen, O. J. Guy, G. Pope, K. S. Teng, T. Maffeis, S. P. Wilks, P. A. Mawby, T. Jenkins, A. Brieva, and D. J. Hayton, Mater. Sci. Forum **457-460**, 1337 (2004).
[15] P. Reinke, D. Rudmann, and P. Oelhafen, Phys. Rev. B **61**, 16967 (2000).
[16] Y. Hijikata, H. Yaguchi, Y. Ishida, M. Yoshikawa, T. Kamiya, and S. Yoshida, Mater. Sci. Forum **457-460**, 1341 (2004).
[17] C. Önneby and C. G. Pantan, J. Vac. Sci. Technol. A **15**, 1597 (1997).
[18] V. V. Afanas'ev, M. Bassler, G. Pensl, and M. Schulz, Phys. Status Solidi A **162**, 321 (1997).
[19] L. I. Johansson, C. Virojanadara, T. Eickhoff, and W. Drube, Mater. Sci. Forum **433-436**, 539 (2003).
[20] Y. Ishida, T. Takahashi, H. Okumura, T. Jikimoto, H. Tsuchida, M. Yoshikawa, Y. Tomioka, M. Midorikawa, Y. Hijikata, and S. Yoshida, Mater. Sci. Forum **389-393**, 1013 (2002).
[21] R. Krause-Rehberg and H. S. Leipner, *Positron Annihilation in Semiconductors*, (Springer, Berlin, 1998), p. 27.
[22] M. J. Puska and R. M. Nieminen, Rev. Mod. Phys. **66**, 841 (1994).
[23] P. J. Schultz and K. G. Lynn, Rev. Mod. Phys. **60**, 701 (1988).
[24] A. Uedono, S. Tanigawa, and Y. Ohji, Phys. Lett. A **133**, 82 (1988).
[25] P. Asoka-Kumar, K. G. Lynn, and D. O. Welch, J. Appl. Phys. **76**, 4935 (1994).
[26] T. C. Leung, P. Asoka-Kumar, B. Nielsen, and K. G. Lynn, J. Appl. Phys. **73**, 168 (1993).
[27] M. Clement, J. M. M. de Nijs, P. Balk, H. Schut, and A. van Veen, J. Appl. Phys. **81**, 1943 (1997).
[28] R. Suzuki, T. Ohdaira, A. Uedono, and Y. Kobayashi, Appl. Surf. Sci. **194**, 89 (2002).
[29] G. Brauer, W. Anwand, W. Skorupa, A. G. Revesz, and J. Kuriplach, Phys. Rev. B **66**, 195331 (2002).
[30] M. Maekawa, A. Kawasuso, M. Yoshikawa, and H. Itoh, Appl. Surf. Sci. **216**, 365 (2003).
[31] M. Maekawa, A. Kawasuso, M. Yoshikawa, and A. Ichimiya, Mater. Sci. Forum **457-460**, 1301 (2004).
[32] J. Dekker, K. Saarinen, H. Ólafsson, and E. Ö. Sveinbjörnsson, Appl. Phys. Lett. **82**, 2020 (2003).
[33] K. Ueno, Phys. Status Solidi A **162**, 299 (1997).
[34] K. G. Lynn, J. R. MacDonald, R. A. Boie, L. C. Feldman, J. D. Gabbe, M. F. Fobbins, E. Bonderup, and J. Golovchenko, Phys. Rev. Lett. **38**, 241 (1977).
[35] P. Asoka-Kumar, M. Alatalo, V. J. Ghosh, A. C. Kruseman, B. Nielsen, and K. G. Lynn, Phys. Rev. Lett. **77**, 2097 (1996).
[36] R. Suzuki, Y. Kobayashi, T. Mikado, H. Ohgaki, M. Chiwaki, T. Yamazaki, and T. Tomimasu, Jpn. J. Appl. Phys., Part 1 **30**, 532 (1991).
[37] P. Kirkegaard, N. Pederson, and M. Eldrup, PATFIT-88, Riso-M-2704, 1989.
[38] M. Alatalo, H. Kauppinen, K. Saarinen, M. J. Puska, J. Mäkinen, P. Hautojärvi, and R. M. Nieminen, Phys. Rev. B **51**, 4176 (1995).
[39] E. Clementi and C. Roetti, At. Data Nucl. Data Tables **14**, 177 (1974).

[40] G. Kresse and J. Hafner, Phys. Rev. B **47**, R558 (1993).
[41] J. Sarnthein, A. Pasquarello, and R. Car, Phys. Rev. Lett. **74**, 4682 (1995).
[42] E. Boroński and R. M. Nieminen, Phys. Rev. B **34**, 3820 (1986).
[43] M. J. Puska, S. Mäkinen, M. Mannien, and R. M. Nieminen, Phys. Rev. B **39**, 7666 (1989).
[44] X. Gonze, J.-M. Beuken, R. Caracas, F. Detraux, M. Fuchs, G.-M. Rignanese, L. Sindic, M. Verstraete, G. Zerah, F. Jollet, M. Torrent, A. Roy, M. Mikami, Ph. Ghosez, J.-Y. Raty, and D. C. Allan, Comput. Mater. Sci. **25**, 478 (2002).
[45] A. van Veen, H. Schut, J. de Veries, R. A. Hakvoort, and M. R. Ijpma, AIP Conf. Proc. **218**, 171 (1990).
[46] A. Uedono, L. Wei, S. Tanigawa, and Y. Ohji, Jpn. J. Appl. Phys., Part 1 **33**, 3330 (1994).
[47] H. L. Au, P. Asoka-Kumar, B. Nielsen, and K. G. Lynn, J. Appl. Phys. **73**, 2972 (1993).
[48] M. Hasegawa, M. Tabata, T. Miyamoto, Y. Nagashima, T. Hyodo, M. Fujinami, and S. Yamaguchi, Mater. Sci. Forum **175-178**, 269 (1995).
[49] M. Eldrup, D. Lightbody, and J. N. Sherwood, Chem. Phys. **63**, 51 (1981).
[50] A. S. Saleh, J. W. Taylor, and P. C. Rice-Evans, Appl. Surf. Sci. **149**, 87 (1999).
[51] Z. Q. Chen, M. Maekawa, S. Yamamoto, A. Kawasuso, X. L. Yuan, T. Sekiguchi, R. Suzuki, and T. Ohdaira, Phys. Rev. B **69**, 035210 (2004).
[52] M. Hasegawa, M. Tabata, M. Fujinami, Y. Ito, H. Sunaga, S. Okada, and S. Yamaguchi, Nucl. Instrum. Methods Phys. Res. B **116**, 347 (1996).
[53] M. Hasegawa, M. Saneyasu, M. Tabata, Z. Tang, Y. Nagai, T. Chiba, and Y. Ito, Nucl. Instrum. Methods Phys. Res. B **166-167**, 431 (2000).
[54] J. Kuriplach, W. Anwand, G. Brauer, and W. Skorupa, Appl. Surf. Sci. **194**, 84 (2002).
[55] U. Myler, R. D. Goldberg, A. P. Knights, D. W. Lawther, and P. J. Simpson, Appl. Phys. Lett. **69**, 3333 (1996).
[56] J. Kuriplach, M. Šob, G. Brauer, W. Anwand, E. M. Nicht, P. G. Coleman, and N. Wagner, Phys. Rev. B **59**, 1948 (1999).
[57] P. Asoka-Kumar, Mater. Sci. Forum **255-257**, 166 (1997).
[58] J. Dekker, R. Aavikko, and K. Saarinen, Appl. Surf. Sci. **194**, 97 (2002).
[59] Y. Nagai, T. Nonaka, M. Hasegawa, Y. Kobayashi, C. L. Wang, W. Zheng, and C. Zhang, Phys. Rev. B **60**, 11863 (1999).
[60] Z. Tang, T. Nonaka, Y. Nagai, and M. Hasegawa, Mater. Sci. Forum **363-365**, 67 (2001).
[61] T. Miyagoe, M. Fujinami, T. Sawada, R. Suzuki, T. Ohdaira, and T. Akahane, Mater. Sci. Forum **445-446**, 150 (2004).
[62] M. H. Weber, K. G. Lynn, B. Barbiellini, P. A. Sterne, and A. B. Denison, Phys. Rev. B **66**, 041305(R) (2002).
[63] H. Saito, Y. Nagashima, T. Hyodo, and T. Chang, Phys. Rev. B **52**, R689 (1995).
[64] M. J. Puska and C. Corbel, Phys. Rev. B **38**, 9874 (1988).
[65] H. Li, S. Dimitrijev, D. Sweatman, H. B. Harrison, P. Tanner, and B. Feil, J. Appl. Phys. **86**, 4316 (1999).
[66] Y. Hijikata, H. Yaguchi, M. Yoshikawa, and S. Yoshida, Mater. Sci. Forum **389-393**, 1033 (2002).
[67] P. Jamet and S. Dimitrijev, Appl. Phys. Lett. **79**, 323 (2001).
[68] A. Ekoué, O. Renault, T. Billon, L. D. Cioccio, and G. Guillot, Mater. Sci. Forum **433-436**, 555 (2003).
[69] I. Trimaille, J. Ganem, I. C. Vickridge, S. Rigo, G. Battistig, E. Szilagyi, I. J. Baumvol, C. Radtke, and F. C. Stedile, Nucl. Instrum. Methods Phys. Res. B **219-220**, 914 (2004).